Journal of
Materials Chemistry C

Materials for optical, magnetic and electronic devices

Accepted Manuscript

This article can be cited before page numbers have been issued, to do this please use: J. Guo, C. zheng, K. Ke, M. Zhang, H. Yang, J. Zhao, Z. He, H. Lin, S. Tao and X. Zhang, *J. Mater. Chem. C*, 2020, DOI: 10.1039/D0TC04751A.

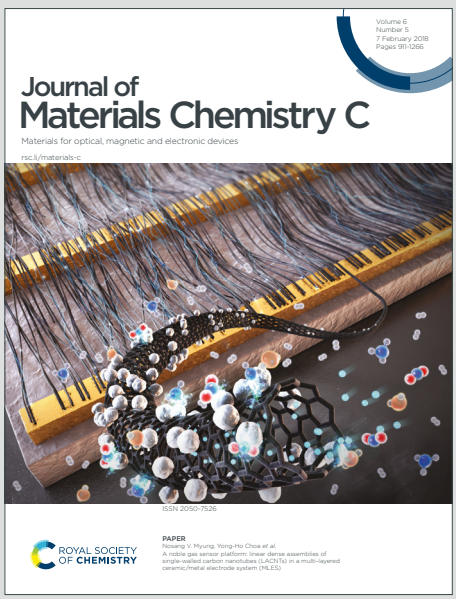

ROYAL SOCIETY OF CHEMISTRY

rsc.li/materials-c

View Article Online
DOI: 10.1039/D0TC04751A

ARTICLE

Novel triazine derivatives with deep LUMO energy levels as the electron-accepting components of exciplexes

Received 00th October 2020,
Accepted 00th October 2020

DOI: 10.1039/x0xx00000x

Jing-Guo, [a] Cai-Jun Zheng, *[a] Ke Ke, [a,b] Ming Zhang, [a,b] Hao-Yu Yang, [a] Jue-Wen Zhao, [a] Ze-Yu He, [a] Hui Lin, [a] Si-Lu Tao, *[a] and Xiao-Hong Zhang [b]

Although a variety of electron-accepting molecules (Acceptors) have been reported to develop exciplexes, their LUMO energy levels are still limited within -2.9 to -3.3 eV. Such a narrow range seriously restricts the development of exciplexes. In this work, three novel triazine-based Acceptors, 2,4-diphenyl-6-(3-(phenylsulfonyl) phenyl)-1,3,5-triazine (TRZ-1SO_2), 2-phenyl-4,6-bis(3-(phenylsulfonyl) phenyl)-1,3,5-triazine (TRZ-2SO_2) and 2,4,6-tris(3-(phenylsulfonyl) phenyl)-1,3,5-triazine (TRZ-3SO_2) were developed with deep LUMO energy levels of -3.38, -3.58 and -3.74 eV, respectively. Particularly, the TRZ-3SO_2 exihits the deepest LUMO energy level of -3.74 eV among reported Acceptors so far. Combining with electron-donating molecule 1,3-bis(9,9-dimethylacridin-10(9H)-yl) benzene (13AB), three exciplexes 13AB:TRZ-1SO_2, 13AB:TRZ-2SO_2 and 13AB:TRZ-3SO_2 were constructed with the emission from green to orange-red. The OLED using 13AB:TRZ-3SO_2 as the emitter exhibits an orange-red emission peaking at 572 nm with the maximum external quantum efficiency of 5.5%. Meanwhile, green and red phosphorescent OLEDs (PhOLEDs) were fabricated with interfacial exciplex hosts by combining these Acceptors with 4,4'-bis(carbazole-9-yl) biphenyl (CBP), which successfully exhibit superior performance than reference devices. These results demonstrate that three novel Acceptors have great potential in the development of exciplexes.

Introduction

Exciplexes have attracted enormous attention in the organic light-emitting diode (OLED) field in recent years due to their natural thermally activated delayed fluorescence (TADF) characteristic.[1-5] Formed between electron-donating and electron-accepting molecules (Donor and Acceptor), exciplexes are characterized with intermolecular charge-transfer (CT) transition, and their highest occupied molecular orbital (HOMO) and lowest unoccupied molecular orbital (LUMO) are located on Donor and Acceptor, respectively.[6-8] Therefore, exciplexes possess completely separated frontier molecular orbitals and intrinsically have extremely small energy gaps (ΔE_{ST}s) between their S_1 and T_1 energy levels,[9] which will promote the reverse intersystem crossing process and theoretically realize the full utilization of triplet excitons.[10-12] Furthermore, the constituting Donor and Acceptor generally possess hole- and electron-transporting properties, respectively, thus exciplexes are also natural bipolar mixed systems.[13] The balanced carriers-transporting can be even achieved by adjusting the mixing ratio between Donor and Acceptor, which is beneficial to simplify the device structures and improve device performance.[14-16] Therefore, exciplexes are widely reported as the TADF emitters and hosts of OLEDs in recent years.[17-21] Till now, exciplex-based OLEDs have achieved significant progress and show great application prospects. However, they still have to solve two main problems. First, the photoluminescence quantum yields (PLQYs) of exciplex emitters are relatively low, especially for red exciplex emitters. Meanwhile, the stabilities of exciplex-based OLEDs need further improvement. Thus, to meet the requirements of commercialized OLEDs, it is still urgent to improve the performance of exciplex-based OLEDs by developing new exciplex systems.

According to our previous researches, the formations and energy gaps of exciplexes are mainly depended on the HOMO energy level of Donor and the LUMO energy level of Acceptor.[22-25] Thus, abundant candidates of Donor and Acceptor are crucial for the development of exciplexes. As common electron-donating groups, like triarylamine, carbazole, phenoxazine, and acridine possess the evidently different electron-donating ability, the HOMO energy levels of current Donors can vary in a large range from -5.1 to -6.1 eV.[26-31] Reversely, although the Acceptors have also been developed based on different electron-withdrawing groups, such as pyridine, phenanthroline, pyrimidine, triazine, phenylphosphine oxide and so on, their LUMO energy levels are generally limited within -2.9 to -3.3 eV.[32-35] Such a narrow range seriously restricts the development of exciplexes, till now, most reported exciplexes have energy gaps over 2.3 eV with blue, green or yellow emission.[36-39] To address this issue, it is essential to develop new Acceptors with deeper LUMO energy levels.

Among familiar electron-withdrawing groups, triazine exhibits relatively deep LUMO energy level and stable

[a] School of Optoelectronic Science and Engineering, University of Electronic Science and Technology of China, Chengdu 610054, P. R. China.
[b] Institute of Functional Nano & Soft Materials (FUNSOM), Soochow University, Suzhou 215123, P. R. China.

† Electronic Supplementary Information (ESI) available. See DOI:10.1039/x0xx00000x

electrochemical properties. In this work, we worked on triazine derivatives to develop new Acceptors. To further lower their LUMO energy levels, diphenyl sulfone group, which also has strong electronegativity and good electron-transporting property, was introduced into the molecules with different numbers. And three novel triazine-based Acceptors, 2,4-diphenyl-6-(3-(phenylsulfonyl) phenyl)-1,3,5-triazine (TRZ-1SO_2), 2-phenyl-4,6-bis(3-(phenylsulfonyl) phenyl)-1,3,5-triazine (TRZ-2SO_2) and 2,4,6-tris(3-(phenylsulfonyl) phenyl)-1,3,5-triazine (TRZ-3SO_2) were developed. TRZ-1SO_2, TRZ-2SO_2 and TRZ-3SO_2 successfully exhibit deep LUMO energy levels of -3.38, -3.58 and -3.74 eV, respectively. The LUMO energy level of -3.74 eV is almost the deepest among all reported Acceptors so far. By using 1,3-bis(9,9-dimethylacridin-10(9H)-yl) benzene (13AB) as the Donor, three exciplexes 13AB:TRZ-1SO_2, 13AB:TRZ-2SO_2 and 13AB:TRZ-3SO_2 were constructed with the emission from green to orange-red. And the OLED using 13AB:TRZ-3SO_2 as the emitter exhibits an orange-red emission peaking at 572 nm with the maximum external quantum efficiency (EQE) of 5.5%. To make full use of these new Acceptors, we further constructed interfacial exciplex hosts in the OLEDs by combining these Acceptors with 4,4'-bis(carbazole-9-yl) biphenyl (CBP). And the green and red phosphorescent OLEDs (PhOLEDs) successfully exhibit superior performance compared with the 3,3'-(5'-(3-(pyridin-3-yl) phenyl)-[1,1':3',1''-terphenyl]-3,3''-diyl) dipyridine (TmPyPB)-based contrastive devices. We believe the remarkable performance of these devices effectively proves the great prospects of three new Acceptors in the development of exciplexes.

Experimental Section/Methods

General Information

All materials were purchased from commercial suppliers and used without further purification. The ^{1}H- and ^{13}C-NMR spectra were respectively measured by using Bruker AV-400 and AV-600 NMR spectrometers to clarify the molecular structures of synthesized Acceptors. High-resolution mass spectra were obtained by using a WATERS mass spectrometer. Differential scanning calorimetry (DSC) measurements were performed on a NETZSCH DSC204 calorimeter at a heating rate of 5 ℃ min^{-1} from 50 to 200 ℃ under a nitrogen atmosphere. Thermogravimetric analysis (TGA) was performed on a TAQ 500 thermogravimeter by measuring the weight loss while heating from 50 to 550 ℃ under nitrogen atmosphere. Absorption and PL spectra were measured using a Hitachi UV–vis spectrophotometer U-3010 and a Hitachi F-4600 fluorescence spectrometer, respectively. The single-molecule and mixed constituting molecules in dichloromethane or chlorobenzene were spin-coated on quartz glass and annealed at 100 °C for 10 min to form films. Their phosphorescence spectra were measured at 77 K using a Hitachi F-4600 fluorescence spectrometer. Cyclic voltammetry was performed by using a CHI660E electrochemical analyzer. A Pt disk, Pt wire, and Ag were used as the working, counter, and reference electrodes, respectively. The 0.1 MBu_4NPF_6 and ferrocenium/ferrocene (Fe^+/Fe) were applied as supporting electrolyte and standard material, respectively. The reduction potentials of ETMs were conducted in DMF.

OLEDs Fabrication

The patterned ITO substrates (135 nm,15 Ω square^{-1}) were cleaned with detergent and deionized water, then dried in an oven at 120 °C for two hours, treated with UV-ozone for 30 minutes. All materials were deposited by vacuum evaporation in a base pressure of about 5 × 10^{-4} Pa. The evaporation rates of all the materials were monitored by quartz crystals. Organic materials were deposited at a rate of less than 1.5 Å s^{-1} and the LiF and Al were deposited at the rates of 0.1 and 10 Å s^{-1}, respectively. The current density-voltage curves were obtained by using a Keithley 2400 source meter. The EL spectrum and CIE color coordinates were measured by a Spectra scan PR655 photometer. The EQE of devices was calculated from the current density, luminance, and EL spectrum, assuming a Lambertian distribution. All the measurements were performed in ambient conditions.

Materials and Synthesis

All commercially available reagents and solvents were used without further purification.

Synthesis of 2,4-diphenyl-6-(3-(phenylsulfonyl) phenyl)-1,3,5-triazine (TRZ-1SO_2). A mixture of 2(3-Bromophenyl)-4,6-diphenyl-1,3,5-triazine (5 mmol, 1.94 g) and sodium benzenethiolate (6 mmol, 793 mg), potassium t-butoxide (10 mmol, 1.12 g) was added to a two-port reaction flask. Then, add 80 ml of DMF solvent under N_2 protection, refluxed at 150 °C for 20 h. After the reaction is completed, it is cooled to room temperature, the organic phase is extracted with a large amount of water and dichloromethane, and dried over anhydrous sodium sulfate. Finally, the product was purified by column chromatography using petroleum ether and dichloromethane. After drying, a white gummy solid B1was obtained (1.52 g, 73% yield); ^{1}H NMR (400 MHz,$CDCl_3$) δ 8.60-8.52 (m, 4H), 8.21 (dt, J = 7.5, 1.6 Hz, 1H), 7.62 (t, J = 1.5 Hz, 1H), 7.54 (t, J =7.5 Hz, 1H), 7.48 (dp, J = 5.6, 2.0 Hz, 6H), 7.45 (dt, J = 7.5, 1.5 Hz, 1H), 7.42-7.35 (m, 2H), 7.35-7.29 (m, 2H), 7.29-7.22 (m, 1H). MS (EI) m/z: calcd for $C_{27}H_{19}N_3S$ ([M]$^+$), 417.53; found, 417.21.

Add product B1 (1.52g), 10 ml of hydrogen peroxide and 80 ml of acetic acid solution to a 200 ml round bottom flask, reflux at 108 °C to carry out oxidation reaction. After 6 h of reaction, it was cooled to room temperature, filtered, and finally recrystallized from petroleum ether to remove impurities to obtain 1.38 g of white solid TRZ-1SO_2 (84% yield); ^{1}H NMR (400 MHz, $CDCl_3$) δ 9.31 (t, J = 1.8 Hz, 1H), 8.96 (dd, J = 7.8, 1.6 Hz, 1H), 8.78-8.74 (m, 4H), 8.15 (dd, J = 7.8, 1.7 Hz, 1H), 8.07-8.03 (m, 2H), 7.72 (t, J = 7.9 Hz, 1H), 7.66 - 7.62 (m, 2H), 7.61-7.57 (m, 6H), 7.56-7.52 (m, 1H).^{13}C NMR (151 MHz, $CDCl_3$) δ 171.90, 169.96, 142.46, 141.41, 137.79, 135.69, 133.39, 132.85, 131.06, 129.72, 129.41, 129.05, 128.72, 127.97, 127.85. MS (EI) m/z: calcd for $C_{27}H_{19}N_3O_2S$ ([M]$^+$), 449.97; found, 450.21. Anal. Calcd. for $C_{27}H_{19}N_3O_2S$ (%): C, 72.14; H, 4.26; N, 9.35; O,7.12; S, 7.13. Found: C, 72.21; H, 4.19; N, 9.42; O, 7.02; S, 7.16.

View Article Online
DOI: 10.1039/D0TC04751A

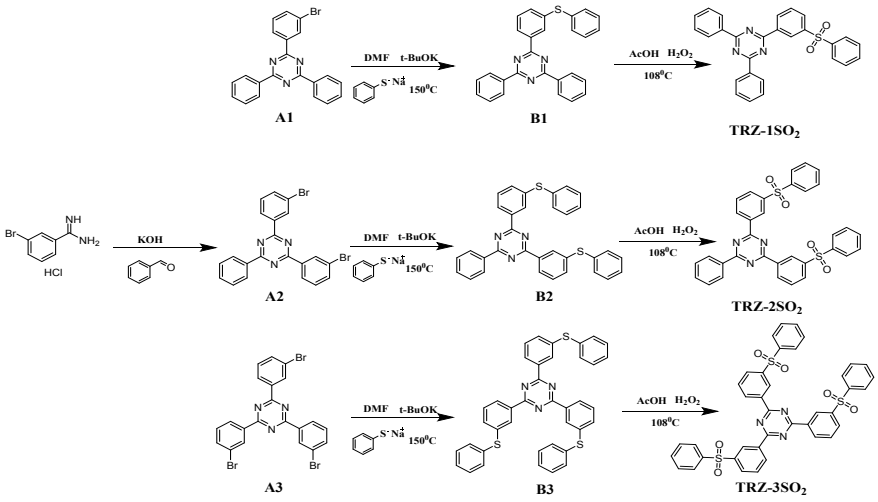

Scheme 1. Synthesis of TRZ-1SO_2, TRZ-2SO_2, and TRZ-3SO_2.

Synthesis of 2-phenyl-4,6-bis(3-(phenylsulfonyl) phenyl)-1,3,5-triazine (TRZ-2SO_2). Add 3-bromobenzamide hydrochloride (10 mmol, 2.35 g) and KOH solid (15 mmol, 0.84 g) to a 200 ml single-mouth reaction flask, 80 ml of ethanol as solvent, and finally, add 0.5 ml of benzaldehyde with a syringe. The mixture was stirred at room temperature for 8 hours. When the milky white suspension appeared in the reaction liquid, the stirring was stopped. Filtered and dried to give 1.82 g of a white solid A2 (yield 78%); ^{1}H NMR (400 MHz, $CDCl_3$) δ 8.60-8.51 (m, 2H), 8.30 (dt, J = 7.5, 1.5 Hz, 2H), 7.64-7.57 (m, 4H), 7.53-7.43 (m, 3H), 7.38 (t, J = 7.5 Hz, 2H). MS (EI) m/z: calcd for $C_{21}H_{13}Br_2N_3$ ($[M]^+$), 467.16; found, 466.98.

A mixture of solid A2 (3.9 mmol, 1.82 g) and sodium benzenethiolate (11.7 mmol, 1.54 g), potassium t-butoxide (7.8 mmol, 875 mg) was added to a 200 ml two-port flask and place in the reaction station. The reaction solution was stirred while adding 50 ml of DMF solvent under N_2 protection, refluxed at 150 °C for 20 h after the reaction is completed, cooled to room temperature. Then extracted the organic phase with a large amount of water and dichloromethane and dried with anhydrous sodium sulfate, evaporated, and purified by column chromatography using petroleum ether and dichloromethane to give a white gummy solid B2 (1.25g, yield 61%); ^{1}H NMR (400 MHz, $CDCl_3$) δ 8.59-8.53 (m, 2H), 8.20 (dt, J = 7.5, 1.6 Hz, 2H), 7.60 (t, J = 1.5 Hz, 2H), 7.56-7.43 (m, 7H), 7.41-7.30 (m, 8H), 7.25-7.17 (m, 2H). MS (EI) m/z: calcd for $C_{33}H_{23}N_3S_2$ ($[M]^+$), 525.69; found, 525.26.

The product B2 (1.25 g) was added in a 200 ml round bottom flask, 10 ml of hydrogen peroxide and 80 ml of acetic acid solution were also added, and the mixture was heated to reflux at 108 °C to carry out an oxidation reaction. After 6 hours, it was cooled to room temperature, filtered, and recrystallized with petroleum ether to remove impurities, and finally 1.04 g of a white solid TRZ-2SO_2 was obtained (yield 74%); ^{1}H NMR (400 MHz, $CDCl_3$) δ 9.28 (t, J=1.7 Hz, 2H), 8.94 (dq, J=7.8, 1.4 Hz, 2H), 8.75 (dt, J=8.6, 1.5 Hz, 2H), 8.18 (ddt, J=7.8, 2.0, 1.1 Hz, 2H), 8.09-8.05 (m, 4H), 7.74 (t, J = 7.8 Hz, 2H), 7.68-7.65 (m, 1H), 7.63-7.54 (m, 8H). ^{13}C NMR (151 MHz, $CDCl_3$) δ 167.52, 165.52, 137.90, 136.52, 132.46, 130.37, 128.75, 128.61, 128.53, 126.58, 125.13, 124.76, 124.40, 124.10, 123.30, 123.12.MS (EI) m/z: calcd for $C_{33}H_{23}N_3O_4S_2$ ($[M]^+$), 589.68; found, 589.95. Anal. Calcd. for $C_{33}H_{23}N_3O_4S_2$ (%): C, 67.22; H, 3.93; N, 7.13; O, 10.85; S, 10.87. Found: C, 67.37; H, 4.04; N, 7.11; O, 10.69; S, 10.79.

Synthesis of 2,4,6-tris(3-(phenylsulfonyl) phenyl)-1,3,5-triazine (TRZ-3SO_2). TRZ-3SO_2 was synthesized in the same way as TRZ-1SO_2, except that the reaction material was changed to 2,4,6-tris(3-bromophenyl) -1,3,5-triazine. The final product was purified and dried to give a white solid (0.85g, 53% yield); ^{1}H NMR (400 MHz, Chloroform-d) δ 9.26 (d, J =2.0 Hz, 3H), 8.92 (d, J =7.8 Hz, 3H), 8.20 (d, J = 7.8 Hz, 3H), 8.08 (dd, J = 7.6, 2.0 Hz, 6H), 7.76 (t, J = 7.8 Hz, 3H), 7.59 (d, J = 7.2 Hz, 9H). ^{13}C NMR (151 MHz, $CDCl_3$) δ 170.69, 142.88, 141.13, 136.70, 133.58, 133.42, 131.62, 120.02, 129.59, 128.22, 127.90. MS (EI) m/z: calcd for $C_{39}H_{27}N_3O_6S_3$($[M]^+$), 729.84; found, 729.95. Anal. Calcd. for $C_{39}H_{27}N_3O_6S_3$ (%): C, 64.18; H, 3.73; N, 5.76; O, 13.15; S, 13.18. Found: C, 63.95; H, 3.84; N, 5.87; O, 13.09; S, 13.25.

Results and discussion

Design and Synthesis of Acceptors

The synthetic routes of TRZ-1SO_2, TRZ-2SO_2, and TRZ-3SO_2 are shown in **Scheme 1**. These materials were prepared in similar synthesis steps. B1, B2, and B3 were prepared by the nucleophilic addition reaction of thiophenol sodium with corresponding bromo compounds A1, A2, and A3 respectively, where A2 was prepared via the heterocyclic addition reaction of 3-bromobenzamide hydrochloride with benzaldehyde. Then all of the intermediates were oxidized to obtain final compounds of TRZ-1SO_2, TRZ-2SO_2, and TRZ-3SO_2. The final compounds were further purified by sublimation and confirmed by ^{1}H NMR,^{13}C NMR, mass spectrometry, and elemental analysis (detail shown in Supporting Information). [40]

Theoretical Calculation

To reveal the influence of the sulfone group on the frontier molecular orbitals and excited states of three new Acceptors,

density functional theory (DFT) calculations have been performed in Gaussian program at the B3LYP/6-31G (d) level. The theoretical HOMO and LUMO distributions of three Acceptors are depicted in **Figure S1a**. It is shown that the LUMOs are mainly dispersed on triphenyltriazine core, while HOMOs gradually transfer from triphenyltriazine to diphenylsulfone for TRZ-1SO_2, TRZ-2SO_2 and TRZ-3SO_2, respectively. These results should be ascribed to the strong conjugations between triazine core and diphenylsulfone unit, enhancing the electron deficiency of triazine core from TRZ-1SO_2 to TRZ-3SO_2.[41] The strong conjugations are also confirmed by the small twisted angles between the triazine core and diphenylsulfone branch as shown in Figure S1b. As shown in Figure S1c, the theoretical values of HOMO, LUMO, S_1 and T_1 energy levels were also calculated for three Acceptors. It can be observed that these Acceptors exhibit almost same S_1/ T_1 energy levels, while their HOMO and LUMO energy levels get deeper as the number of diphenylsulfone unit increases.

Thermal Properties

The thermal properties of all Acceptors were measured by thermogravimetric analysis (TGA) and differential scanning calorimetry (DSC) under nitrogen atmosphere.[42] As shown in **Figure S2**, TRZ-1SO_2, TRZ-2SO_2 and TRZ-3SO_2 exhibit excellent thermal stability with high decomposition temperature (T_d) of 352, 436 and 477 °C, respectively. As the T_d is positively related to the molecular weight, T_ds of three new Acceptors are improved greatly with the increase of diphenylsulfone units. And no obvious glass transition temperature (T_g) is observed in the range from 25 to 200 °C for all three Acceptors, which indicates these compounds are not easy to crystallize.[43] Consequently, those Acceptors are ideal and excellent for the vacuum deposition process.

Table 1. The physicochemical properties of TRZ-1SO_2, TRZ-2SO_2, and TRZ-3SO_2.

Acceptors	λ_{abs}[a] (nm)	λ_{PL}[b] (nm)	λ_{Phos}[c] (nm)	Eg[d] (eV)	HOMO/LUMO (eV)	T_1[e] (eV)	T_d (℃)
TRZ-1SO_2	370	412	420	3.35	-6.73/-3.38	2.95	352
TRZ-2SO_2	375	412	420	3.30	-6.88/-3.58	2.95	436
TRZ-3SO_2	378	412	420	3.28	-7.02/-3.74	2.95	477

[a] Determined from the absorption band edges of their toluene solution at room temperature; [b] Determined from the first peak of fluorescent spectra of their toluene solution at room temperature; [c] Determined from the first phosphorescent emission peak of their dimethyl tetrahydrofuran solution at 77 K; [d] Calculated from their absorption band edge; [e] Estimated from the first peak of phosphorescence spectrum at 77K.

Electrochemical and Carrier Transporting Properties

To determine the frontier molecular orbitals energy levels of three Acceptors, their electrochemical properties were measured by cyclic voltammetry (CV) in dimethyl formamide (DMF) under nitrogen atmosphere.[44] As presented in **Figure 1**, all Acceptors exhibit quasi-reversible reduction curves. And the LUMO energy levels determined from the onset of reduction waves were -3.38, -3.58 and -3.74 eV for TRZ-1SO_2, TRZ-2SO_2 and TRZ-3SO_2, respectively, as referred to the redox couple of ferrocenes. It can be observed that as the number of sulfone groups increases, the LUMO energy levels of the Acceptors get deeper. And the value of -3.74 eV is almost the deepest LUMO energy level among all reported Acceptors.[45] We believe these new Acceptors with deep LUMO energy levels will benefit to develop various exciplexes. Deduced from the LUMO values and the absorption edges, the HOMO energy levels of three compounds were -6.73, -6.88 and -7.02 eV for TRZ-1SO_2, TRZ-2SO_2 and TRZ-3SO_2, respectively.

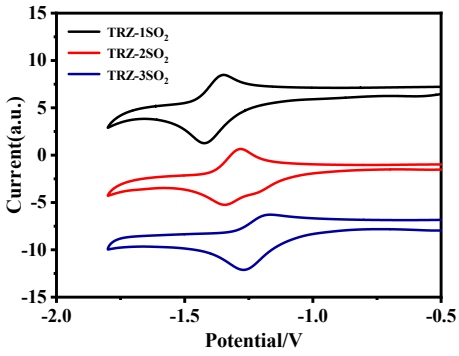

Figure 1. The Cyclic voltammograms of TRZ-1SO_2, TRZ-2SO_2 and TRZ-3SO_2.

To study the electron-transporting properties of these Acceptors, electron-only devices were fabricated with the structure of ITO/Al (30 nm)/LiF (1 nm)/ETL (100 nm)/LiF (1 nm)/Al (100 nm). In these devices, LiF is used as a buffer layer between the organic layer and the electrode. The ETL of these devices were TmPyPB, TRZ-1SO_2, TRZ-2SO_2, and TRZ-3SO_2, respectively. Electric-field dependent mobilities evaluated by using the space charge-limited current (SCLC) method are presented in **Figure S3**. The electron mobilities of TmPyPB, TRZ-1SO_2, TRZ-2SO_2 and TRZ-3SO_2 are varied within the range from 2.7×10^{-5} to 3.5×10^{-5} $cm^2\ v^{-1}\ s^{-1}$, 1.6×10^{-6} to 6.1×10^{-6} $cm^2\ v^{-1}\ s^{-1}$, 7.3×10^{-6} to 1.2×10^{-5} $cm^2\ v^{-1}\ s^{-1}$ and 1.1×10^{-5} to 3.1×10^{-5} $cm^2\ v^{-1}\ s^{-1}$, respectively with fields varying from 6.4×10^5 V cm^{-1} to 1.0×10^6 V cm^{-1}. Meanwhile, with more sulfone groups, TRZ-2SO_2 and TRZ-3SO_2 exhibit better electron mobilities than TRZ-1SO_2.

Photophysical Properties

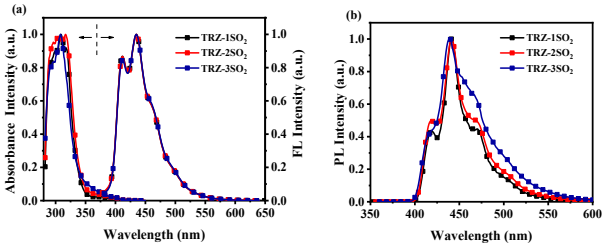

Figure 2. (a) UV-vis absorption and fluorescence spectra (excited at 360 nm) of TRZ-1SO_2, TRZ-2SO_2, TRZ-3SO_2 in toluene solutions at room temperature; (b) Phosphorescence spectra (excited at 340 nm) of TRZ-1SO_2, TRZ-2SO_2, TRZ-3SO_2 in dimethyl tetrahydrofuran solution at 77 K.

View Article Online
DOI: 10.1039/D0TC04754A

To determine the photophysical properties of TRZ-1SO_2, TRZ-2SO_2 and TRZ-3SO_2, the ultraviolet-visible (UV-vis) absorption and photoluminescence (PL) spectra were investigated in toluene solutions at room temperature. As shown in **Figure 2a**, all Acceptors exhibit strong absorptions around 310 nm in toluene solution, which can be ascribed to the local excited transitions. From the absorption band edges, the energy band gaps (E_g) of TRZ-1SO_2, TRZ-2SO_2 and TRZ-3SO_2 are assumed to be 3.35, 3.30 and 3.28 eV, respectively. And the fluorescence (FL) spectra of TRZ-1SO_2, TRZ-2SO_2 and TRZ-3SO_2 are the same in the whole range, including two peaks at 412 and 435 nm, in accord with their similar electronic states. The phosphorescent spectra of three Acceptors measured in dimethyl tetrahydrofuran solution at 77 K were shown in **Figure 2b**, and the triplet energy levels (T_1s) of TRZ-1SO_2, TRZ-2SO_2 and TRZ-3SO_2 were all estimated as 2.95 eV, calculated from the first peak of their phosphorescence spectra.[46] The detailed physicochemical data are summarized in **Table 1**.

Exciplex Emitters Based on New Acceptors

Since an exciplex formation requires an efficient charge transfer between Donor and Acceptor, it is important to select an appropriate Donor combined with these Acceptors.[47] Here, 13AB is selected as the Donor, three exciplexes 13AB:TRZ-1SO_2, 13AB:TRZ-2SO_2 and 13AB:TRZ-3SO_2 were constructed. And their photophysical properties were investigated in thin films at room temperature. As shown in **Figure S4**, all systems exhibit nearly identical absorption spectra to those of the constituting molecules, and no new absorption band appears at longer wavelengths, suggesting that there exists no formation of new ground-state transition in the mixed films.[48] And the PL spectra of mixed films exhibit typical exciplex characteristics with a peak at 507, 538 and 554 nm respectively, which is significantly redshifted and broadened relative to those of the constituting molecules. Moreover, the PLQYs of three exciplex emitters were also measured in nitrogen atmosphere, and their values are 56.3% for 13AB:TRZ-1SO_2, 41.8% for 13AB:TRZ-2SO_2 and 25.4% for 13AB:TRZ-3SO_2, respectively. The decrease of the PLQY values is because the non-radiative transition will be enhanced with the decrease of energy gap for exciplex emitters.

To evaluate the capability of using 13AB:Acceptors (TRZ-1SO_2, TRZ-2SO_2 and TRZ-3SO_2) as TADF emitters in the OLEDs, three devices E1-E3 were fabricated with a simple structure: ITO/TAPC (40 nm)/13AB (10 nm)/EML (30 nm)/Acceptor (45 nm)/LiF (1 nm)/Al (100 nm). In these devices, ITO and LiF/Al are used as the anode and the cathode, respectively. TAPC is used as the hole-injection layer. 13AB and Acceptor are used as the hole-transporting layer and electron-transporting layer,[49] respectively. 13AB:Acceptor with a weight ratio of 1:1 is used as the EML. **Figure 3a** shows the device structure and schematic diagram of the energy levels of materials used in devices. And the chemical structures of the materials used in this paper are depicted in **Figure S5**.

Figure 3b-e display the electroluminescence (EL) characteristics of these devices, and the performance data are summarized in **Table 2**. Device E1-E3 exhibit low turn-on voltage about 2.1-2.3 V. And the turn-on voltages of E2 and E3 are slightly lower than that of E1 due to the deeper-lying LUMO energy level of TRZ-2SO_2 and TRZ-3SO_2. The emission maxima of the EL spectra are 532, 548, and 572 nm for E1, E2, and E3, respectively, which corresponds to the green, yellow, and orange-red emission, respectively. As the LUMO energy levels of three Acceptors deepen with the increase of diphenylsulfone units, the EL spectra are gradually red-shifted with the smaller energy gaps. And obviously, each of the EL spectra does not agree to any monomer emission, its exciplex characteristic is confirmed again.[50] As shown in **Figure S6**, the EL spectra of three devices are almost independent with the increased driving voltages, indicating stable exciplex emission. In addition, as shown in Figure 3c and 3e, the OLED using 13AB:TRZ-3SO_2 as the emitters exhibits an orange-red emission peaking at 572 nm with the maximum EQE of 5.5%. The remarkable performance of devices effectively proves the great prospects of these Acceptors in the development of exciplexes.

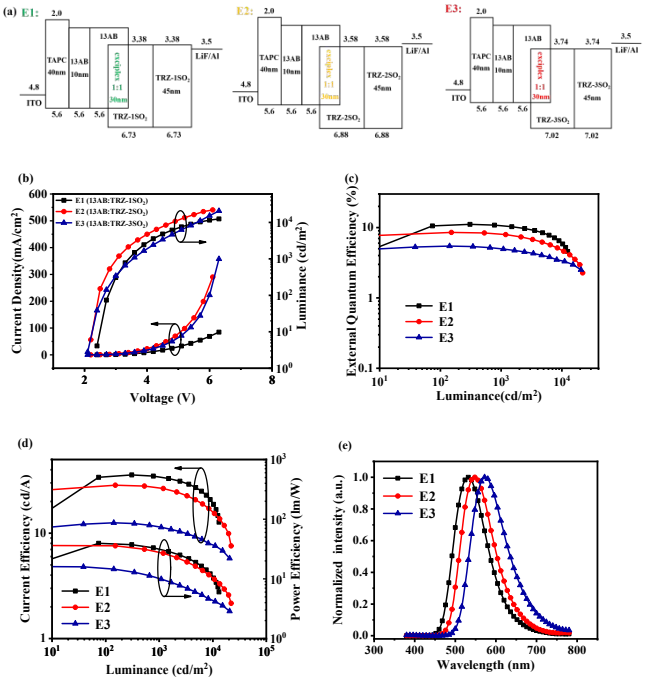

Figure 3. (a) device structures, energy level diagram of used materials in exciplex-based OLEDs. the EL characteristics of exciplex-based OLEDs: (b) current density-voltage-luminance curves; (c) EQE-luminance curves; (d) current efficiency-luminance-power efficiency and (e) EL spectra.

Exciplex hosts Based on New Acceptors

To make full use of three new Acceptors, we further constructed interfacial exciplex hosts in the OLEDs by combining these Acceptors with CBP.[51] The absorption and PL spectra of CBP, Acceptors and CBP:Acceptors in thin films are displayed in **Figure S7**. The PL spectra of mixed films show representative exciplex characteristics, which are observably red-shifted and broadened in comparison to those of the constituent parts.[52] Before utilizting as the hosts, the EL spectra of exciplexes formed between CBP and three Acceptors were first measured. And Device E4-E6 were fabricated with a structure of ITO/TAPC

View Article Online
DOI: 10.1039/D0TC04751A

Table 2. Electroluminescence of Data for Devices E1-E3, G1-G4, and R1-R4.

Device	V_{on}[a] (V)	CE_{max} (cd/A)	PE_{max} (lm/W)	EQE_{max} (%)	PE, EQE_{100}[b] (lm/W, %)	PE, EQE_{500}[c] (lm/W, %)	λ_{max} (nm)	CIE[d]
E1	2.3	35.7	37.4	11.1	39.0, 10.7	35.1, 10.6	532	(0.33, 0.57)
E2	2.1	28.5	35.8	8.5	35.9, 8.4	31.6, 8.0	548	(0.40, 0.60)
E3	2.1	12.5	14.6	5.5	14.9, 5.4	12.0, 5.0	572	(0.49, 0.51)
G1	2.5	88.6	106	23.2	84. 1, 23. 0	63.7, 21.2	524	(0.32, 0.64)
G2	2.4	85.9	108	22.7	80.9, 21.1	53.8, 17.1	524	(0.32, 0.64)
G3	2.2	55	44.3	14.8	49.5, 14.5	41.9, 14.7	524	(0.32, 0.64)
G4	2.9	75.8	65.2	20.0	63.8, 18.6	61.2, 19.8	524	(0.32, 0.64)
R1	2.92	36.6	32.1	23.1	21.2, 22.8	15.8, 21.9	612	(0.62, 0.38)
R2	2.66	40.8	47.4	24.4	24.4, 20.1	15.9, 17.0	608	(0.61, 0.39)
R3	2.69	30.6	29	18.6	22.6, 18.6	17.0, 17.8	604	(0.61, 0.39)
R4	3.29	32.2	27.1	22.4	22.0, 22.4	17.8, 21.8	612	(0.63, 0.37)

[a] Turn-on voltage at 1 cd/m^2; [b] PE and EQE at a brightness of 100 cd/m^2; [c] PE and EQE at a brightness of 500 cd/m^2; [d] CIE coordinate at 1000 cd m^{-2}

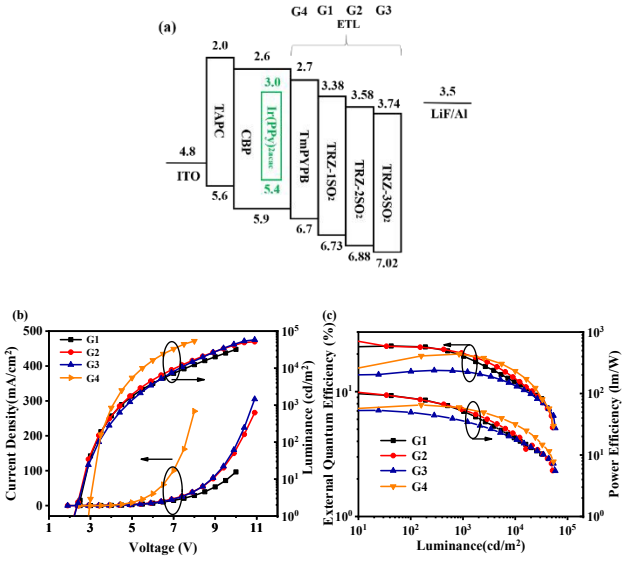

Figure 4. (a) device structures, energy level diagram of used materials in green devices based on CBP/Acceptors interfacial exciplex hosts. the EL characteristics of green devices: (b) current density-voltage-luminance curves; (c) EQE-luminance-power efficiency curves.

(40 nm)/CBP (20 nm)/EML (30 nm)/Acceptor (45 nm)/LiF (1 nm)/Al (100 nm), where CBP:Acceptor with a weight ratio 1:1) is used as the EML. As shown in **Figure S8,** all EL spectra of three CBP-based exciplexes are consistent with their PL spectra with peaks at 468, 512 and 528 nm for CBP:TRZ-1SO_2, CBP:TRZ-2SO_2 and CBP:TRZ-3SO_2, respectively. These results indicated CBP:TRZ-1SO_2 and CBP:TRZ-2SO_2 have high enough energy levels to sensitize green phosphorescent emitters, while CBP:TRZ-3SO_2 can't. Then green and red phosphorescent devices are fabricated by using interfacial exciplexes CBP/Acceptor as the hosts. The structure of green devices (Device G1-G3) is as follows: ITO/TAPC (40 nm)/CBP: Ir(PPy)$_2$acac (8 wt%, 30 nm)/Acceptor (45 nm)/LiF(1 nm)/Al (100 nm). For comparison, Device G4 was fabricated under the same structure except for using TmPyPB as an Acceptor.

Figure 4a shows the device structure and schematic diagram of the energy levels of materials used in devices. As shown in **Figure 4b**, G1-G3 exhibit lower turn-on voltage than G4, which should be attributed to the superiority of interfacial exciplex hosts.[53] In G4, without interfacial exciplex formed between CBP and TmPyPB, the excitons should be formed on CBP. While in G1-G3 with interfacial exciplex hosts, the excitons are directly formed between the LUMO energy level of Acceptor and the HOMO energy level of CBP, corresponding to lower energy gaps.[54] Therefore, CBP/Acceptor interfacial exciplex hosts exhibit lower turn-on voltages than CBP single host. Nevertheless, as TmPyPB has higher electron mobility than three new Acceptors, the driving voltages of TmPyPB-based device are lower than other devices. From **Figure S9**, all the devices exhibit a single emission peak wavelength at around 524 nm, which indicates that the energy transfers from hosts to emitters. As presented in **Figure 4c**, G1-G2 exhibit higher maximum PEs respectively of 106 and 108 lm W^{-1} than G4, which should be ascribed to their low turn-on voltages and high maximum EQEs of 23.2% and 22.7%, respectively. Meanwhile, G3 shows the lowest maximum EQE of 14.8%, which is because CBP/TRZ-3SO_2 can't fully harvest all excitons to Ir(PPy)$_2$acac.[55]

View Article Online
DOI: 10.1039/D0TC04751A

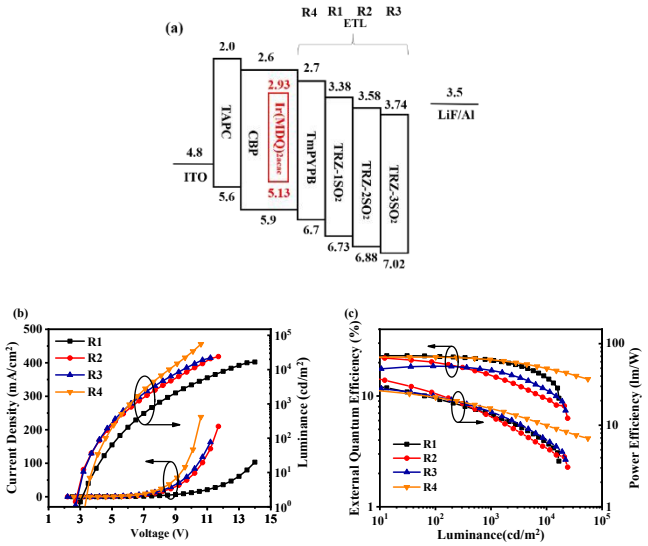

Figure 5. (a) device structures, energy level diagram of used materials in green devices based on CBP/Acceptors interfacial exciplex hosts. the EL characteristics of green devices: (b) current density-voltage-luminance curves; (c) EQE-luminance-power efficiency curves.

Red phosphorescent OLEDs were fabricated with the similar structure: ITO/TAPC (40 nm)/CBP: $Ir(MDQ)_2acac$ (6 wt%, 30 nm)/Acceptor (70 nm)/LiF (1nm)/Al (100 nm), where Acceptor was TRZ-$1SO_2$, TRZ-$2SO_2$, TRZ-$3SO_2$, and TmPyPB, respectively (Device R1-R4). The device structure and schematic diagram of the energy levels of each layer and EL characteristics are exhibited in **Figure 5**. It can be observed that R1-R3 exhibit higher maximum PEs (32.1, 47.4, and 29 lm W^{-1}, respectively) than R4, which can be attributed to their low turn-on voltages and high maximum EQEs. Particularly, R3 exhibits the poor performance of the lowest maxium EQE of 18.6% comparing to R1 and R2. It can be explained by EL spectra displayed in **Figure S10**. The EL spectrum of R3 not only shows emission maximum centered at 604 nm but also an obvious bulge around 520 nm that is attributed to the emission of CBP/TRZ-$3SO_2$ exciplex. Thus, the energy is not completely transferred from host to emitter, leading to the lowest EQE.[56-58] The detailed performance data of green and red devices are summarized in **Table 2**.

Conclusions

In summary, three novel triazine-based Acceptors (TRZ-$1SO_2$, TRZ-$2SO_2$ and TRZ-$3SO_2$) were designed and synthesized. All Acceptors exhibit deep LUMO energy levels, in which TRZ-$3SO_2$ shows the deepest LUMO energy level of -3.74 eV among Acceptors reported so far. Three exciplex-based OLEDs from green to orange-red were fabricated by employing these Acceptors and 13AB. The OLED using 13AB:TRZ-$3SO_2$ as the TADF emitter exhibits an orange-red emission peaking at 572 nm with the maximum EQE of 5.5%. Furthermore, three interfacial exciplex hosts were formed between these Acceptors and CBP to develop red and green phosphorescent OLEDs. All PhOLEDs exhibit higher PEs and lower driving voltages, significantly better than TmPyPB-based contrastive devices. The outstanding performance of these devices not only suggests the great potential of three new Acceptors for the development of exciplex emitters but also proves the superiority of interfacial exciplex hosts to develop high-performance PhOLEDs.

Conflicts of interest

There are no conflicts to declare.

Acknowledgements

The acknowledgements come at the end of an article after the conclusions and before the notes and references. This work was supported by the National Natural Science Foundation of China (Grant Nos. 51773029, 61775029 and 51533005), the Fundamental Research Funds for the Central Universities (Grant No. ZYGX2016Z010) and the International Cooperation and Exchange Project of Science and Technology Department of Sichuan Province (Grant Nos. 2019YFH0057 and 2019YFH0059).

Notes and references

1 X. Cai, W. Qiu, M. Li, B. Li, Z. Wang, X. Wu, D. Chen, X. Jiang, Y. Cao and S.-J. Su, *Adv. Opt. Mater.*, 2019, **7**, 1801554.
2 M. Chapran, P. Pander, M. Vasylieva, G. Wiosna-Salyga, J. Ulanski, F. B. Dias and P. Data, *ACS Appl. Mater. Interfaces*, 2019, **11**, 13460-13471.
3 K. Goushi, K. Yoshida, K. Sato and C. Adachi, *Nat. Photonics*, 2012, **6**, 253.
4 W. Y. Hung, G. C. Fang, S. W. Lin, S. H. Cheng, K. T. Wong, T. Y. Kuo and P. T. Chou, *Mater. Chem. Front.*, 2020, **4**, 2029-2039.
5 W. Y. Hung, G. C. Fang, S. W. Lin, S. H. Cheng, K. T. Wong, T. Y. Kuo, P. T. Chou, *Sci. Rep.*, 2014, **4**, 5161.
6 S. K. Jeon, H. J. Jang and J. Y. Lee, *Adv. Opt. Mater.*, 2019, **7**, 1801462.
7 M. Mamada, G. Tian, H. Nakanotani, J. Su and C. Adachi, *Angew. Chem. Int. Ed.*, 2018, **57**, 12380.
8 Z. Wang, M. Li, L. Gan, X. Cai, B. Li, D. Chen and S. J. Su, *Adv. Sci.*, 2019, **6**, 1802246.
9 M. Colella, P. Pander, D. S. Pereira and A. P. Monkman, *ACS Appl. Mater. Interfaces*, 2018, **10**, 40001.
10 W. Liu, J.-X. Chen, C.-J. Zheng, K. Wang, D.-Y. Chen, F. Li, Y.-P. Dong, C.-S. Lee, X.-M. Ou and X.-H. Zhang, *Adv. Funct. Mater.*, 2016, **26**, 2002.
11 Y. J. Pu, Y. Koyama, D. Otsuki, M. Kim, H. Chubachi, Y. Seino, K. Enomoto and N. Aizawa, *Chem. Sci.*, 2019, **10**, 9203.
12 M. Zhang, W. Liu, C. J. Zheng, K. Wang, Y. Z. Shi, X. Li, H. Lin, S. L. Tao and X. H. Zhang, *Adv. Sci.*, 2019, **6**, 1801938.
13 S. K. Jeon, K. S. Yook and J. Y. Lee, *Nanotechnol.*, 2016, **27**, 224001.
14 C. S. Oh, Y. J. Kang, S. K. Jeon and J. Y. Lee, J. *Phys. Chem. C*, 2015, **119**, 22618.
15 Q. Wang, Q.-S. Tian, Y.-L. Zhang, X. Tang and L.-S. Liao, *J. Mater. Chem. C*, 2019, **7**, 11329.
16 D. Zhang, M. Cai, Y. Zhang, Z. Bin, D. Zhang and L. Duan, *ACS Appl. Mater. Interfaces*, 2016, **8**, 3825.
17 C.-Y. Huang, S.-Y. Ho, C.-H. Lai, C.-L. Ko, Y.-C. Wei, J.-A. Lin, D.-G. Chen, T.-Y. Ko, K.-T. Wong, Z. Zhang, W.-Y. Hung and P.-T. Chou, *J. Mater. Chem. C*, 2020, **8**, 5704.
18 B. Liang, J. Wang, Y. Cui, J. Wei and Y. Wang, *J. Mater. Chem. C*, 2020, **8**, 2700.

19 H. Lim, H. Shin, K. H. Kim, S. J. Yoo, J. S. Huh and J. J. Kim, *ACS Appl. Mater. Interfaces*, 2017, **9**, 37883.
20 R. Sheng, A. Li, F. Zhang, J. Song, Y. Duan and P. Chen, *Adv. Opt. Mater.*, 2019, **8**, 1901247.
21 H. Shin, S. Lee, K.-H. Kim, C.-K. Moon, S.-J. Yoo, J.-H. Lee and J.-J. Kim, *Adv. Mater.*, 2014, **26**, 4730.
22 R. Braveenth, H. W. Bae, I. J. Ko, W. Qiong, Q. P. B. Nguyen, P. G. S. Jayashantha, J. H. Kwon and K. Y. Chai, *Org. Electron.*, 2017, **51**, 463.
23 Z. Hu, W. Fu, L. Yan, J. Miao, H. Yu, Y. He, O. Goto, H. Meng, H. Chen and W. Huang, *Chem. Sci.*, 2016, **7**, 5007.
24 S.-J. Su, C. Cai and J. Kido, *J. Mater. Chem.*, 2012, **22**, 3447.
25 Z. Yang, B. Xu, J. He, L. Xue, Q. Guo, H. Xia and W. Tian, *Org. Electron.*, 2009, **10**, 954.
26 W. Y. Hung, P. Y. Chiang, S. W. Lin, W. C. Tang, Y. T. Chen, S. H. Liu, P. T. Chou, Y. T. Hung and K. T. Wong, *ACS Appl. Mater. Interfaces*, 2016, **8**, 4811.
27 J. Jia, L. Zhu, Y. Wei, Z. Wu, H. Xu, D. Ding, R. Chen, D. Ma and W. Huang, *J. Mater. Chem. C*, 2015, **3**, 4890.
28 H. Sasabe, D. Tanaka, D. Yokoyama, T. Chiba, Y.-J. Pu, K.-i. Nakayama, M. Yokoyama and J. Kido, *Adv. Funct. Mater.*, 2011, **21**, 336.
29 C. H. Shih, P. Rajamalli, C. A. Wu, W. T. Hsieh and C. H. Cheng, *ACS Appl. Mater. Interfaces*, 2015, **7**, 10466.
30 S.-J. Yoo, H.-J. Yun, I. Kang, K. Thangaraju, S.-K. Kwon and Y.-H. Kim, *J. Mater. Chem. C*, 2013, **1**, 2217.
31 P. Zassowski, P. Ledwon, A. Kurowska, A. P. Herman, M. Lapkowski, V. Cherpak, Z. Hotra, P. Turyk, K. Ivaniuk, P. Stakhira, G. Sych, D. Volyniuk and J. V. Grazulevicius, *Dyes Pigm.*, 2018, **149**, 804.
32 W. Y. Hung, G. C. Fang, Y. C. Chang, T. Y. Kuo, P. T. Chou, S. W. Lin and K. T. Wong, *ACS Appl. Mater. Interfaces*, 2013, **5**, 6826.
33 M. Sarma and K.-T. Wong, *ACS Appl. Mater. Interfaces*, 2018, **10**, 19279.
34 X. Song, D. Zhang, H. Li, M. Cai, T. Huang and L. Duan, *ACS Appl. Mater. Interfaces*, 2019, **11**, 22595.
35 Q.-S. Tian, X.-D. Zhu and L.-S. Liao, *Mater. Chem. Front.*, 2020, **4**, 1648.
36 P. Yuan, X. Guo, X. Qiao, D. Yan and D. Ma, *Adv. Opt. Mater.*, 2019, **7**, 1801648.
37 T. L. Wu, S. Y. Liao, P. Y. Huang, Z. S. Hong, M. P. Huang, C. C. Lin, M. J. Cheng and C. H. Cheng, *ACS Appl. Mater. Interfaces*, 2019, **11**, 19294.
38 M. Zhang, K. Wang, C. J. Zheng, D. Q. Wang, Y. Z. Shi, H. Lin, S. L. Tao, X. Li, X. H. Zhang, Front. Chem. 2019, 7, 16.
39 Y. Hu, Y. J. Yu, Y. Yuan, Z. Q. Jiang and L. S. Liao, *Adv. Opt. Mater.*, 2020, **8**, 1901917.
40 D. M. Sun, X. K. Zhou, J. T. Liu, X. L. Sun, H. H. Li, Z. J. Ren, D. G. Ma, M. R. Bryce and S. K. Yan, *ACS Appl. Mater. Interfaces*, 2015, **7**, 27989-27998.
41 Y. Im, M. Kim, Y. J. Cho, J.-A. Seo, K. S. Yook and J. Y. Lee, *Chem. Mater.*, 2017, **29**, 1946-1963.
42 V. Jankus, C. J. Chiang, F. Dias and A. P. Monkman, *Adv. Mater.*, 2013, **25**, 1455-1459.
43 J.-H. Lee, S.-H. Cheng, S.-J. Yoo, H. Shin, J.-H. Chang, C.-I. Wu, K.-T. Wong and J.-J. Kim, *Adv. Funct. Mater.*, 2015, **25**, 361-366.
44 T. C. Lin, M. Sarma, Y. T. Chen, S. H. Liu, K. T. Lin, P. Y. Chiang, W. T. Chuang, Y. C. Liu, H. F. Hsu, W. Y. Hung, W. C. Tang, K. T. Wong and P. T. Chou, *Nat. Commun.*, 2018, **9**, 3111.
45 T. Liu, G. Xie, C. Zhong, S. Gong and C. Yang, *Adv. Funct. Mater.*, 2018, **28**, 1706088.
46 Y. Seino, H. Sasabe, Y.-J. Pu and J. Kido, *Adv. Mater.*, 2014, **26**, 1612-1616.
47 [S.-J. Su, Y. Takahashi, T. Chiba, T. Takeda and J. Kido, *Adv. Funct. Mater.*, 2009, **19**, 1260-1267.
48 W. Y. Hung, G. C Fang, Y. C. Chang, T. Y. Kuo, P. T. Chou, S. W. Lin and K. T. Wong, *ACS Appl. Mater. Interfaces*, 2013, **5**, 6826-6831.
49 D. Chen, K. Liu, L. Gan, M. Liu, K. Gao, G. Xie, Y. Ma, Y. Cao and S. J. Su, *Adv. Mater.*, 2016, **28**, 6758-6765.
50 X.-K. Liu, Z. Chen, C.-J. Zheng, C.-L. Liu, C.-S. Lee, F. Li, X.-M. Ou and X.-H Zhang, *Adv. Mater.*, 2015, **27**, 2378-2383.
51 M. Cai, T. Xiao, E. Hellerich, Y. Chen, R. Shinar and J. Shinar, *Adv. Mater.*, 2011, **23**, 3590-3596.
52 Y. S. Park, S. Lee, K. H. Kim, S. Y Kim, J. H. Lee and J. J. Kim, *Adv. Funct. Mater.*, 2013, **23**, 4914-4920.
53 J. Zhao, S. Yuan, X. Du, W. Li, C. Zheng, S. Tao and X. Zhang, *Adv. Opt. Mater.*, 2018, **6**, 1800825.
54 E. Ahmed, T. Earmme and S. A. Jenekhe, *Adv. Funct. Mater.*, 2011, **21**, 3889-3899.
55 M. Bian, D. Zhang, Y. Wang, Y.-H. Chung, Y. Liu, H. Ting, L. Duan, Z. Chen, Z. Bian, Z. Liu and L. Xiao, *Adv. Funct. Mater.*, 2018, **28**, 1800429.
56 S. J. Su, H. Sasabe, Y. J. Pu, K. Nakayama and J. Kido, *Adv. Mater.*, 2010, **22**, 3311-3316.
57 H. Ye, D. Chen, M. Liu, S.-J. Su, Y.-F. Wang, C.-C. Lo, A. Lien and J. Kido, *Adv. Funct. Mater.*, 2014, **24**, 3268-3275.
58 D. Zhang, P. Wei, D. Zhang and L. Duan, *ACS Appl. Mater. Interfaces*, 2017, **9**, 19040-19047.

View Article Online
DOI: 10.1039/D0TC04751A

Table of contents

Three novel triazine-based Acceptors with deep LUMO energy levels were successfully developed. TRZ-3SO_2 exihits the deepest LUMO energy level of -3.74 eV. The OLED using 13AB:TRZ-3SO_2 as the emitter exhibits an orange-red emission peaking at 572 nm with the maximum external quantum efficiency of 5.5%.